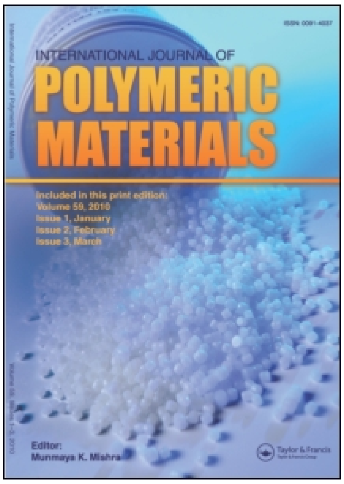

International Journal of Polymeric Materials

Publication details, including instructions for authors and subscription information:
http://www.informaworld.com/smpp/title~content=t713647664

Thermally Stimulated Depolarization Current

Nandika Anne D'souza[a]
[a] Department of Materials Science, University of North Texas, Denton, TX, USA

To cite this Article D'souza, Nandika Anne(2000) 'Thermally Stimulated Depolarization Current', International Journal of Polymeric Materials, 45: 3, 277 — 306

To link to this Article: DOI: 10.1080/00914030008035047

URL: http://dx.doi.org/10.1080/00914030008035047

Intern. J. Polymeric Mater., 2000, Vol. 45, pp. 277–306
Reprints available directly from the publisher
Photocopying permitted by license only

Published by license under
the Gordon and Breach Science
Publishers imprint.
Printed in Malaysia.

Thermally Stimulated Depolarization Current

NANDIKA ANNE D'SOUZA

*Department of Materials Science, University of North Texas,
P.O. Box 305210, Denton, TX 76203, USA*

(Received 18 December 1998)

Thermally stimulated discharge or thermally stimulated polarization and depolarization current is becoming a valuable technique in discerning transitions having a small relaxation strength. Polymer liquid crystals (PLCs) are a group of such materials. This article provides a review of the different experimental techniques associated with the technique and their application to PLCs. Experimental results for thermotropic longitudinal PLCs are presented.

Keywords: Thermally stimulated discharge; thermally stimulated polarization; relaxation strength; polymer liquid crystals; PLCs; thermotropic longitudinal PLCs

1. SCOPE

Thermally stimulated discharge (TSD) refers to the field induced discharge current upon buildup (Thermally Stimulated polarization Current–TSPC) and/or release (Thermally Stimulated Depolarization Current–TSDC) of charges in a dielectric placed between two electrodes. The polarization phenomenon is a consequence of the rotation or migration of charges originating from and remaining within the dielectric. This leads to surface charges which have the opposite polarity to those of the polarizing electrode [1, 2]. Application of the technique of thermally stimulated discharge (TSD) to polymer liquid crystals (PLCs) is driven by three points:

1. the higher mobility of PLCs as compared to other engineering polymers implies longer relaxation times;

2. TSD is a low frequency technique with the estimated experimental frequency given by (10^{-2} to 10^{-4} Hz)[2,1]

$$f = \frac{E_a r}{2\pi R T_m^2} \tag{1}$$

   where E_a is the activation energy, r is the heating rate, R is the ideal gas constant and T_m the temperature of the TSD peak maximum.
3. Dielectric techniques are very promising for investigating PLCs due to their high electric susceptibilities. (see Chapter 3 in this volume)

Conventionally polymer characterization is done through calorimetric, mechanical or dielectric means. To this end a comparison with other techniques is provided in Section 3. Section 4 provides information on instrumentation and experimental techniques. Analytical techniques and theories of cooperative relaxations and the compensation law are provided in Section 5. Applications of TSD to resolve PLC related issues are then presented (Sec. 6). It becomes apparent upon review of literature in this area, that while the potential of this technique is vast, it is still underutilized. To that end, applications to non-PLC systems having potential use in PLCs are also included.

2. INTRODUCTION

Thermally stimulated discharge (TSD) measures the dielectric relaxation of materials through measurement of a field induced thermally stimulated depolarization current (TSDC), also referred to as ionic thermocurrent technique [2]. Under simultaneous application of electric field during a temperature ramp, the orientation of the dipoles results in the formation of an electret. The first electrets were formed by Eguchi [3, 4]. Based on Eq. (1) the effective frequency of operation varies between 10^{-3} – 10^{-5} Hz making it especially suitable for studying systems having long relaxation times.

The use of TSD is in no way limited to polymeric materials. However, since dielectric relaxation is due to hindrance of the motions of the permanent dipoles and free charges by frictional forces, application to polymers has been widespread. TSDC measurements have been traced to Frei and Groetzinger [5] in a review by Vanderschueren and Gasiot [6]. The technique was applied to a series of complex systems by numerous researchers including Gross [7], Wikstroem [8], Gubkin and Matsonashvili [9] and Murphy [10]. Relating these relaxations to fundamental mechanisms of charge storage and release in nonmetallic systems was initiated by Bucci and Fieschi [11]. One of the first detailed investigations on its potential in polymers was initiated by van Turnhout [2, 12]. As Vanderschueren [6] points out, this technique was developed independently by several researchers. It is worthwhile to clarify that TSD is also referred to as electret thermal analysis, thermal current spectra, thermally stimulated depolarization and thermally activated depolarization. Applications to amorphous and semi-crystalline polymers have been reviewed by Bernes *et al.* [13]. The sensitivity of TSD to small fractions of uncured material extends its use to thermosetting systems. In addition, TSD is useful in establishing differences based on tacticity and chemical structure 14, water absorption [15, 16, 17], interfaces in composites [18, 19] *etc.* It's applicability to a wide variety of parameters has been recently reviewed [28].

In another development measurement of the polarization current in TSPC was used to evaluate relaxation behavior of dielectrics [20]. Vanderschuren points out that in the high temperature range, TSPC spectra are usually less well resolved because the relaxational current can be superimposed or masked by the conduction current [21]. Since TSPC does not involve a heating stage prior to data collection, differences between TSPC and TSDC are useful in determining the effects of physical aging, behavior of thermally unstable structures and for revealing non-equilibrium intermediate relaxations.

Both TSDC and TSPC results indicate the cumulative polarization effects of the dielectric. To further isolate individual relaxations related to the macroscopic relaxation, Lacabanne [22] and Chatain [23] proposed a modified TSDC method termed thermal sampling or windowing polarization. They attempted to experimentally deconvolute individual relaxation contributions from the global relaxation spectra.

The first application of the TSD technique in PLCs was conducted by Simon [24] for comb PLCs, in order to estimate the glass transition, degree of mesogenic alignment and degree of stored polarization which is related to their use in optical storage media and non-linear optics.

Recognizing its potential in resolving the complicated chain dynamics associated with PLCs due to the positional and orientational order, Brostow *et al.*, conducted one of the first detailed investigations into the relaxational behavior of longitudinal PLCs [25]. Given the debate surrounding the existence or non existence of the relaxation related to the LC rich phase in PLC copolymers, their study resolved issues such as choice of the polarization temperature, effect of increasing field strength and annealing under an electric field for main chain PLCs.

3. COMPARISON OF TSD WITH CALORIMETRIC, DILATOMETRIC, DYNAMIC MECHANICAL TECHNIQUES

Characterization of the relaxational behavior of PLCs has traversed the spectrum of available techniques. TSD and dielectric spectroscopic techniques are far more sensitive in resolving PLC transitions as compared to calorimetric, dilatometric and dynamic mechanical techniques. A comparison of the sensitivity of different techniques in resolving the transitions of a PET/0.6PHB PLC are shown in Figure 1 [26]. Spatial resolution of morphology through Wide Angle X-ray Scattering (WAXS) and polarizing microscopy are commonly conducted. Investigations on the molecular mobility of the liquid crystalline state using NMR have also been conducted [27]. Cao *et al.*, studied PLCs using the DSC and reported on the width of the mesophase transition that extended to the melting point of the PLC [28]. Cassel and Riga applied a thermal cycling of rapid quenching from the melt state to above the glass transition followed by slow cooling within the glass transition regime. A distinct second step was found to be more pronounced with every subsequent thermal cycle. Regardless of the benefits of thermal cycling, it becomes apparent from Figure 1a [26] that the temperature related to the glass transition is for the most part obscured by its breadth is DSC experiments. Sauer reports that this breadth is related to the degree of order of the PLC [29, 30]. Dilatometric experiments based on the TMA and the Gnomix P-V-T apparatus show dominance of only one transition as shown in Figure 1b. However, in the TMA, the expansivity is strongly related to the orientation of the LCs in the PLC. Dynamic Mechanical Analysis done on a modified torsion braid internal friction instrument has shown two transitions for some PLCs [31]. However, in

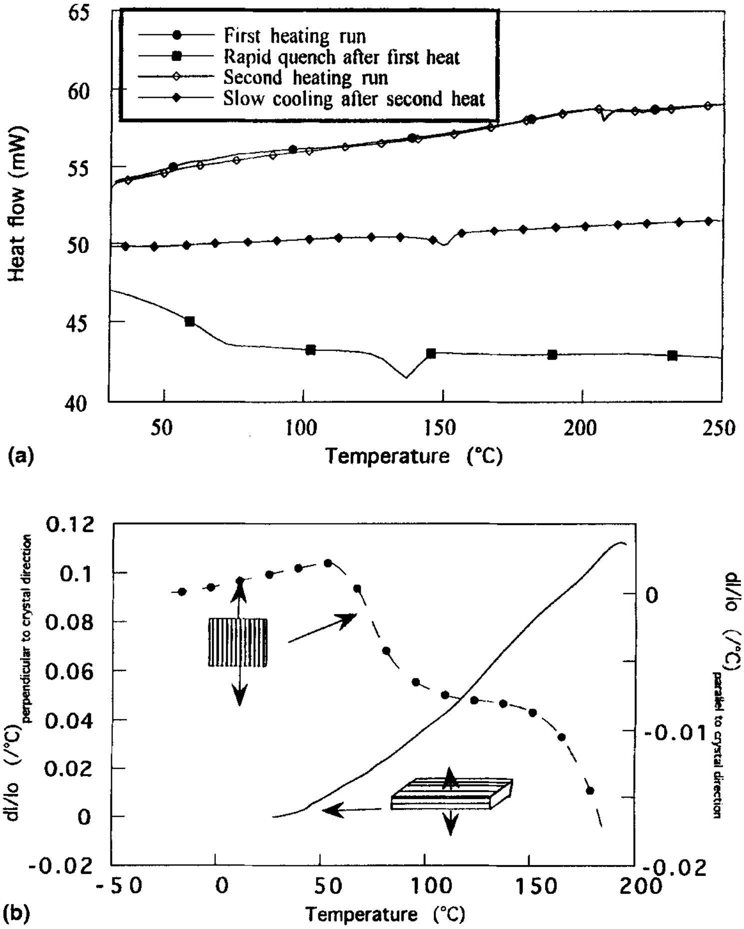

FIGURE 1 Comparison of (a) Differential Scanning Calorimetry and (b) Thermomechanical Analysis of a PET/0.6 PHB longitudinal PLC showing limited T_g resolution of Individual components of the copolymer.

many copolymeric PLCs, an overlap of the transitions is often evident. As shown in the paper by Schönhals and Carius in the same volume, dielectric measurements do reveal two transitions. For the PET/0.6PHB system for instance, dielectric measurements show similar β, α, α' transitions. As can be seen however, the frequency required for distinguishing these multiple transitions is very low. TSD therefore is ideal in resolution of weak transitions in PLC materials.

Probing the temperatures related to the order transitions has required the use of multiple techniques [32]. Multiple techniques are often vital in resolving the nature of the molecular/segmental motions related to a particular transition. Damman *et al.*, for instance studied the dodecylocxy substituted poly(p-phenylene terephthalate)s using both Dielectric spectroscopy (DS) and DMA [33, 34]. Comparison of different techniques indicates that while for engineering polymers the use of dynamic mechanical and dielectric techniques extends the characterization potential for relaxation determination, for PLC materials TSD is more appropriate. The major difficulty using dielectric relaxation spectroscopy of PLCs is that the loss spectra are broad and highly asymmetric with coalescence of the different bands and without clearly resolvable features [6].

4. EXPERIMENTAL

Experimentally the sensitivity of the TSD varies inversely with thickness. While most experiments using TSD have been conducted using solid samples, liquid TSD is also possible. Liquid samples are placed in sample "boats". The holder acts as one electrode. In this case the sample size is $\cong$ 1 ml [35]. Most experimentation on polymers is based on the equipment described by van Turnhout. Commercial systems are available, but in-house build systems are equally common. A typical apparatus would consist of a sample holder that can be used for maintaining an inert atmosphere, a heating unit that can heat at a low rates ($<$ 4 K/min), a dc voltage source, a picoammeter, a thermocouple, and a recording unit either an $X-Y$ chart recorder or a computer connected to the temperature and picoammeter through RS232 ports. Homocharging is avoided by metallizing both sides of the sample.

4.1. Global TSDC Spectra

The essential experimental steps associated with determining the global TSDC spectra are (Fig. 2)

- Heat the polymer to T_p; T_p is higher than the glass transition.
- Apply the electric field, E_p, at $t = t_0$; free charges drift towards the electrodes during this time.

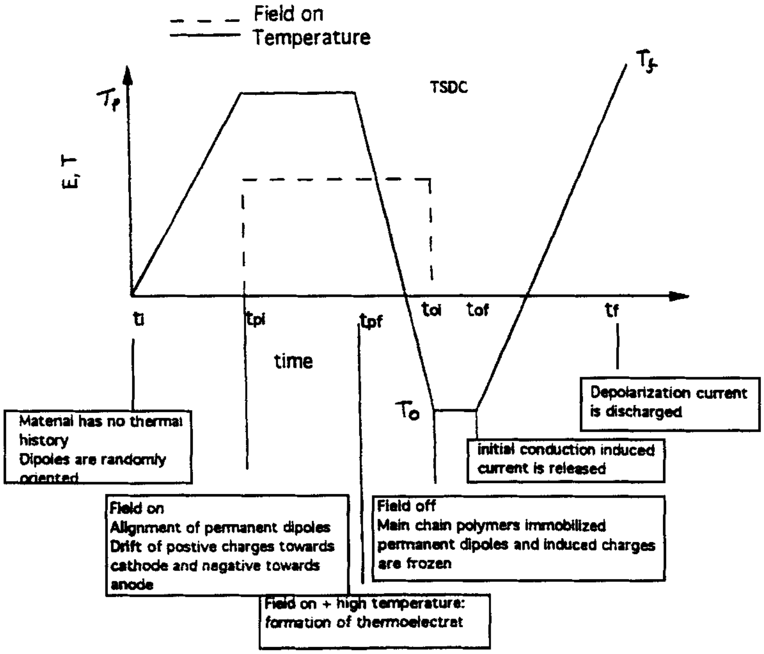

FIGURE 2 Schematic of global TSDC.

- Maintain at $T = T_p$ for time $t_1 - t_0$.
- Cool from $T = T_p$ to $T = T_o$.
- At $T = T_o$ switch electric field off; the material is now a thermoelectret, the.
- After time $t_2 - t_p$ (the thermoelectret is kept shorted to remove stray charges).

The material is heated up to a temperature range where the origins of the polarization relax, the image charges are released from their electrodes and flow towards each other *via* the external circuit. This current is the output measured. In this technique one broad spectra per polarization voltage is obtained. Interaction between different modes of relaxation therefore contribute to broadening of the peaks which need to be individually resolved in information on individual relaxations is known from other techniques. The reorientation occurring at the temperature is dependent on the relaxation time and can be primary (due

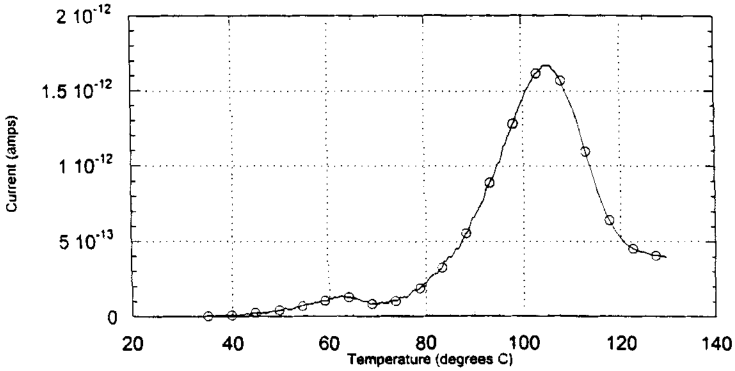

FIGURE 3 Global TSDC spectra of a PET/0.6 PHB showing individual T_g's of the PET rich phase (60°C) and the PHB rich phase (100°C).

to the relaxation of 10 or more repeat units) or secondary (due to the molecular motion of a single repeat unit). A linear relationship between current and field strength is indicative of ohmic behavior. When diffusion of charges takes place, a negative current is often evident.

For a true global spectra, the condition is $T_p \gg T_g$, *i.e.*, and above the upper end of a T_g peak obtained from either the loss spectra of the DMA or the slope change in the DSC thermogram. Partial global spectra are useful when relaxations are close to one another. In that case T_p is taken into the range of T_g. This is followed by two heats, a discharge at T max-5°C and a second heat to $T_{max} + 50°C$ [36, 37]. Figure 3 shows the global relaxation of a PET/0.6PHB liquid crystalline copolymer. Two transitions corresponding to the PET phase (60°C) and PHB phase (100°C) are evident.

Problems encountered in this technique are that the charged species containing some mobility diffuse during the TSD experiment either towards each other through the dielectric or away from the dielectric into the electrode materials, annihilating their charging effects.

4.2. TSDC Window Polarization

Addressing the fact the most polymer relaxations are a cumulative effect of many individual relaxations, Lacabanne [3] and Chatain [4] introduced the technique called "windowing polarization" to study relaxation phenomena. The relaxation time-temperature relationship associated with each window is used to isolate elementary Debye type relaxations of the molecules over the entire relaxation spectrum. Physically, the existence of multiple relaxations can be explained by several mechanisms, including dipole–dipole interactions, variations in size and shape of the rotating dipolar entities, anisotropy of the internal field in which the dipoles reorient (internal rotation, bending and twisting in polymers *etc.*) [6]. This technique is a further development of Bucci *et al.*'s, attempt to isolate overlapping relaxations [38]. To isolate the transitions for a material having two peak temperatures T_{m1} and T_{m2}, they polarized the material at T_{p1} such that $T_{m1} < T_{p1} < T_{m2}$, to allow the dipoles associated with T_{m1} to be polarized but those associated with T_{m2} to be undisturbed. The TSDC curve would then show only the relaxation associated with T_{m1}. The relaxation associated with T_{m2}, could be isolated by polarizing the material at T_{p2} such that $T_{m2} < T_{p1}$ and removing the field at T_d such that $T_{m1} < T_d < T_{m2}$ [6].

A schematic of this technique is shown in Figure 4 and application to a PLC copolymer is shown in Figure 5 [26].

- Sample is polarized at T_p for time t_p (t_p is varied to orient different fractions of the dipoles).
- Sample is quenched to temperature T_d ($T_p - T_d \cong 5-10\,\mathrm{K}$).
- Polarizing field is switched off and T_d maintained for time t_d (depolarization of dipoles that are mobile at or below T_d occurs leaving only dipoles oriented that have mobility in the temperature window of $T_p - T_d$).
- Sample is quenched to $T_o \ll T_d$.
- Sample heated to temperature $T > T_p$ at programmed rate allowing relaxations related to temperature window $T_p - T_d$ to relax.

By doing this at several temperature, a set of individual depolarization curves for each polarization temperature are obtained that are subsets of that obtained by the global TSC spectra. Elementary modes can be isolated and materials relaxation map constructed using window polarization to separate out mixed peaks having small separations has proved useful to also separate the effect of the electret discharge from the glass transition [39].

As reviewed by Ibar *et al.* [40], window polarization and the resultant RMA allows small relaxation differences between a slowly cooled and

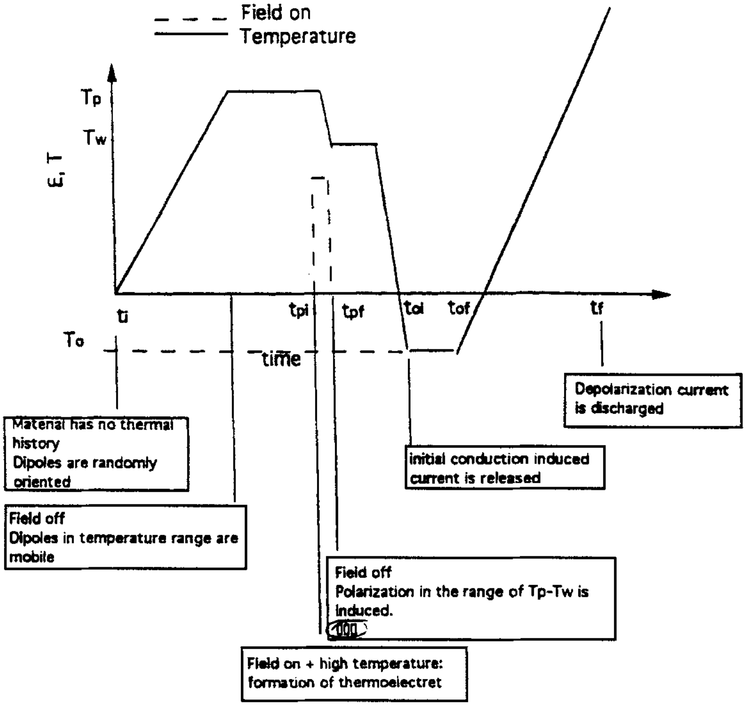

FIGURE 4 Schematic of window polarization technique for determination of relaxation maps.

a quenched plastic, effect of residual stresseds, orientation, degree of cooling, chemical composition and percentage cross-linking to be detected. Analysis of RMA curves is aimed at correlating the simple relaxation modes with the thermokinetic and thermodynamic parameters of the material [41 – 44]. Alternative means of obtaining the T_g are by plotting the enthalpy or entropy *v/s* the polarization temperature and noting the temperature at which the enthalpy is maximum.

Jonscher provided an alternative means for interpreting the individual Debye relaxations similar to that used in deconvolution of dielectric loss spectrum [45]. He noted that the TSD peaks in a non Debye dielectric are broader than the corresponding Debye peaks. In

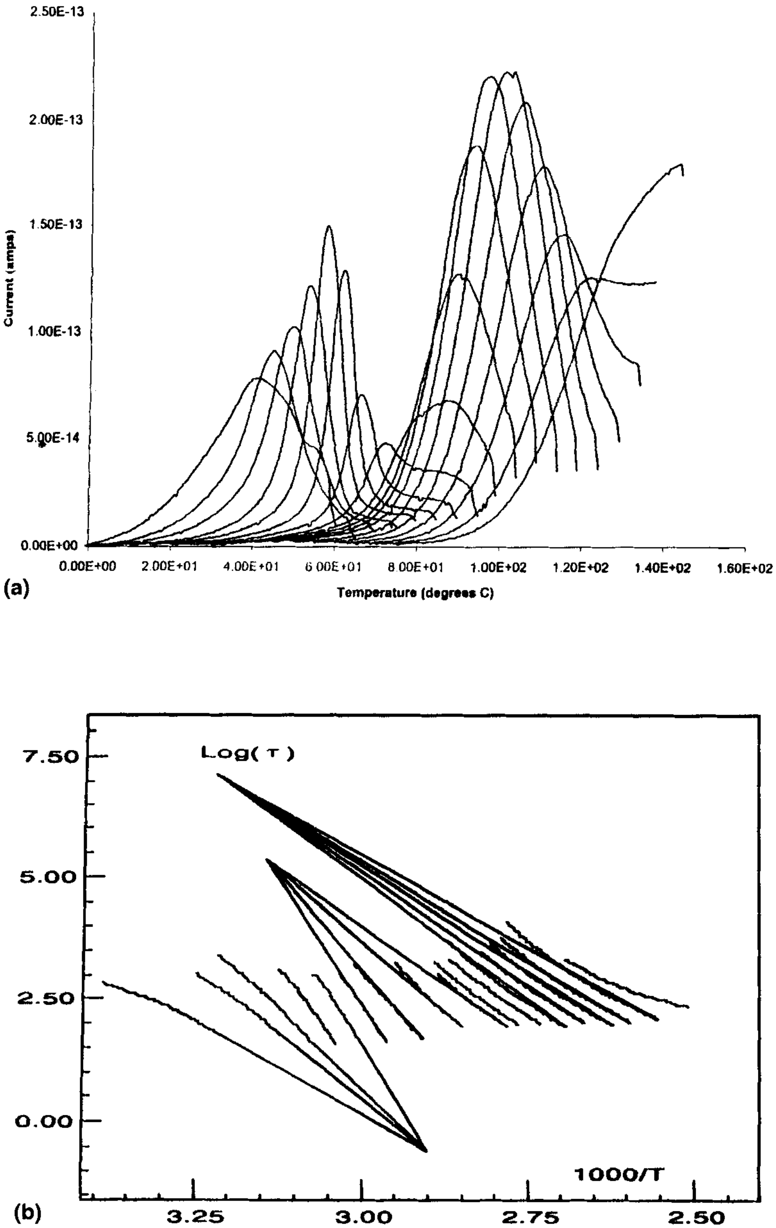

FIGURE 5 Window polarization of a PET/0.6 PHB with (a) peaks due to individual windows and (b) related τ-temperature plots of the individual windows.

conventional TSD analysis this would imply a distribution of activation energies. Secondly the activation energy from the slope of the TSD peak would consistently be lower than that obtained from measuring shifts inducted by different heating rates or by peak shifts in dielectric loss spectra for changing frequency.

4.3. TSPC

Figure 6 shows a schematic of the TSPC experiment with application to a PLC copolymer in Figure 7 [26]. As can be seen only the transition corresponding to the PET phase is evident. Higher temperatures resulted in negative currents. If an unpolarized state is first fixed at low temperature by cooling the sample under short circuit conditions and an electrical field is then applied during subsequent definite heating, the thermally stimulated transition from neutrality to a polarized state can be followed by registering the charging current as a function of temperatures. If dipolar or ionic processes are involved, these show similar peaks as in global TSDC [6, 46]. Further a higher current in

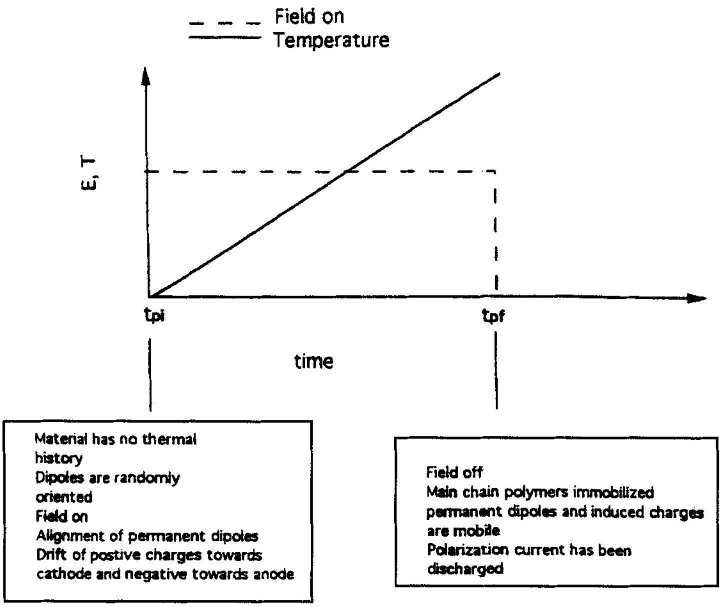

FIGURE 6 Schematic of TSPC.

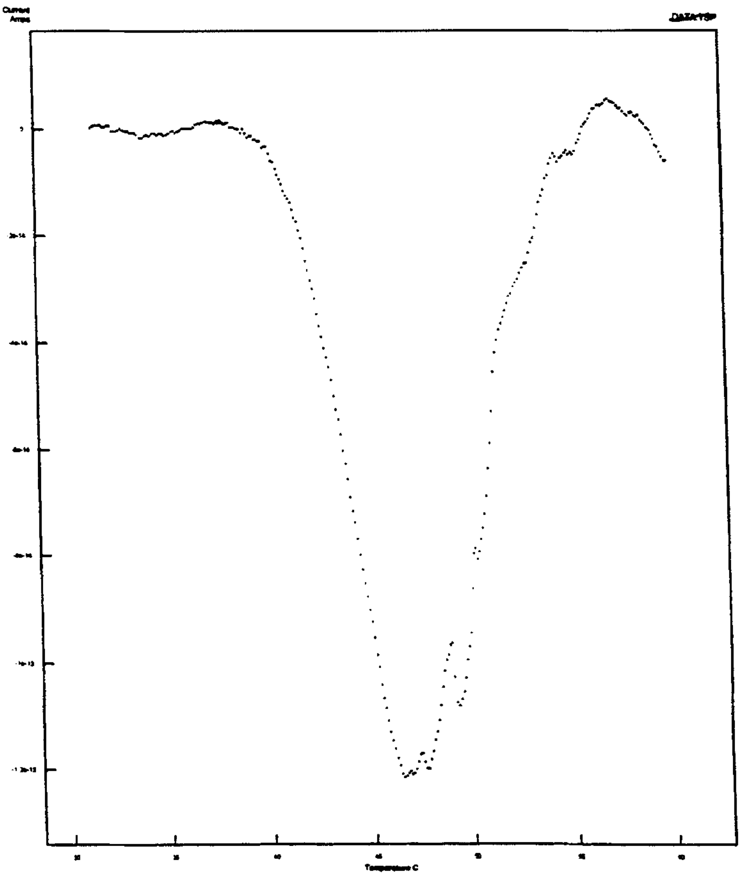

FIGURE 7 TSPC of a PET/0.6 PHB longitudinal PLC.

TSPC; compared to TSDC was related to the formation of ionic space charge during polarization at high temperatures in TSDC [47]. One problem associated with the technique is the danger of obtaining internal conduction or injection currents [6, 48–50].

5. ANALYSIS OF TSD

Global TSDC plots are analyzed based on the total relaxed charge, Q, due to the overall depolarization process is calculated from the area bound by the TSD peak and the abscissa [51] where A is the electrode area and r, the heating rate. Since Q/A is the total polarization P there is a linear relation between the relaxed charge and $\boldsymbol{E}_p$. Plots of current density/electric field v/s temperature depict conductivity.

$$Q = \frac{A}{r}\int_{T_0}^{T_f} i(T)dt \tag{2}$$

Assuming that the relaxation is follows either the Debye (rotational friction) or Frohlich (2 site barrier) model and that the relaxation times for polarization and depolarization are equal, the decay of the polarization is given by:

$$P(t) = P_e \exp\left(-\frac{t}{\tau}\right) \tag{3}$$

where τ is the dipolar relaxation time; P_e is the equilibrium or steady state polarization given by

$$P_e = \frac{sN_d\mu_m^2 E}{kT_\mathrm{p}} \tag{4}$$

where s is the geometrical factor associated with the dipole orientation (for rotating dipoles $s = 1/3$); N_d is the concentration of dipoles; μ_m is the electrical moment; k is Boltzmann's constant and $\boldsymbol{E}_p$ is the directing electrical field operating on the dipoles.

The depolarization current density is given by:

$$i(t) = -\frac{dP(t)}{dt} = \frac{P(t)}{\tau} \tag{5}$$

Since experiments are run under constant rate mode, these equations are modified to include the heating rate. Thus the time is now expressed in terms of the initial temperature, T_l and heating rate, r as

$$t = \frac{(T - T_l)}{r} \tag{6}$$

By assuming a single relaxation time, the relaxation time for the dipoles is obtained through an Arrhenius equation:

$$\tau(T) = \tau_o \exp\left(\frac{E}{kT}\right) \tag{7}$$

For a single relaxation time relaxation, τ_o, is expressed through the Eyring equation as

$$\tau_o = \frac{h}{kT}\left\{\exp - \left(\frac{S}{k}\right)\right\} \tag{8}$$

where S is the activation entropy. Note that this τ_o differs from the Arrhenius pre-factor which is temperature independent.

Lacabanne *et al.*, examined the broad mechanical relaxation of the glass transition in polyolefins. For the relaxation and retardation modes observed around the glass transition temperature, $\tau(t)$ obeys they determined a compensation law [52 – 59] expressed as:

$$\tau(T) = \tau_c \exp\left\{\frac{E}{k}\left(\frac{1}{T} - \frac{1}{T_c}\right)\right\} \tag{9}$$

where τ_c and T_c are the compensation time and temperature respectively. When applied to window polarized experimental results, this implies that the individual relaxations obtained from each window can be coupled to their compensation behavior. A plot of ln $\tau(T)$ *vs* $1/T$ results in an intercept having a value = $\ln(\tau_c) - (E/kT_c)$ and a slope of (E/k). Extrapolation of individual ln τ *vs* $1/T$ plots for each thermal sampling step (or polarization window) produces a single point termed the compensation point. At this compensation temperature, all the discrete processes that constitute the broad relaxation near the glass transition have the same relaxation time.

The compensation law can be examined in conjunction with two empirical equations relating the activation volume to the activation entropy and activation enthalpy [60 – 62].

$$V^* = \frac{\beta S}{\alpha_v} \tag{10}$$

$$V^* = K'\beta E \tag{11}$$

where α_v is the isobaric volumetric expansivity and β is the isothermal compressibility and K' is a constant commonly taken as equal to 4. Since the intercept is in essence an "activation entropy" and the slope is the activation enthalpy one obtains a relationship between the activation entropy and enthalpy by equating these two equations.

$$S = K'\alpha_v E \tag{12}$$

This relationship has been shown to hold for several polymers for relaxational processes related to their glass transition [63]. The Gibbs function is therefore expressed as:

$$G = \frac{\alpha_v V^*}{\beta}\left(\frac{1}{K'\alpha_v} - T\right) \tag{13}$$

Hoffman interpreted TSD spectra by introducing variable mobility of dipoles based on molecular architecture [64] using Eqs. (6) and (7) he studied a series of *n*-paraffins and determined that

$$H = H_{\mathrm{eg}} + n'H_{\mathrm{cs}} \tag{14}$$

$$S = S_{\mathrm{eq}} + n'S_{\mathrm{cs}} \tag{15}$$

where eg = end group contributions and cs = elementary contribution of constitutive segments and n' is the number of segments/molecular chain.

The compensation temperature was therefore obtained from

$$H_{\mathrm{cs}} = T_c^* S_{\mathrm{cs}} \tag{16}$$

Crine derived a thermodynamic model for the compensation law and its physical significance [65, 66]. He returns to the rate theory of Eyring [67] and postulates that the reason that the plots of entropy *v/s* enthalpy obtained from applying the compensation law to individual windows, is due to the reaction free energy. The compensation temperature is interpreted in terms of the Gibbs function being zero or $T_c = 1/K'\ \alpha_v$. Determination of K' is obtained using the Gruneisen constant (a measure of the anharmonicity of vibrations in a solid relation thermal and mechanical properties) defined as

$$\gamma = \frac{\alpha_v V^*}{\beta C_p} \tag{17}$$

Further using the conclusions of Warfield [68] that only the portion of C_p related to interchain vibrations and Sharma's [69–71] relation using the Rao acoustical parameters, Crine determined that the K' value could be given by:

$$K' \cong 2 + (2\alpha_v T)^{-1} + 2/3(\alpha_v T) \tag{18}$$

Equations (6) and (7) must now be rewritten as

$$\tau \cong \frac{h}{kT} \exp\left[\frac{G}{kT}\right] \tag{19}$$

$$\tau \cong \frac{h}{kT} \exp\left(\frac{-S}{k}\right) \exp\left(\frac{H}{kT}\right) \tag{20}$$

substituting the entropy $K'\alpha$ relation one gets

$$\tau \cong \frac{h}{kT} \exp\left[\frac{E}{k}(1 - K'\alpha_v)\right] \tag{21}$$

Activation energy is now obtained from the slope of log (τT) v/s $1/T$. Plotting the enthalpy v/s the entropy it becomes apparent that the intercept is not equal to zero contrary to the prediction of Eq. (11) [26]. Compensation relations for zero entropy are now determined by the non-zero enthalpy intercept denoted as H^* (barrier height for the reverse reaction in the Eyring activated rate formulation). To obtain the compensation coordinates. Crine's relation is:

$$\tau \cong \frac{h}{kT} \exp\left(\frac{H^*}{kT}\right) \exp\left[\frac{E}{k}\left(\frac{1}{T} - K'\alpha_v\right)\right] \tag{22}$$

$$T_c = 1/K'\alpha_v; \tau_c \cong \frac{h}{kT} \exp\left(\frac{H^*}{kT}\right) \tag{23}$$

The temperature dependence of the parameters is related to the nonlinearity in Arrhenius plots. One issue that limits application of this compensation law is the lack of universitality in its occurrence.

Moura Ramos *et al.*, conducted a detailed investigation on the values of the compensation parameters for 960 polymers [72]. Their results further call into question reliance on the relationship between molecular structure and the compensation point.

Whereas, the technique of window polarization has improved the utility of the TSD technique [73], by providing a means to deconvolute Debye relaxation processes from non-Debye relaxation, Aldana used the computerized technique of Direct Signal Analysis based on the theory of Cost [74].

For the high temperature data, the extrapolation is to low temperature and the higher frequency, while for low temperature data the extrapolation is to higher temperature and low frequency. Ibar terms this change as the "*Z* structure". At temperatures lower than the glass transition this restructuring has been attributed to restructuring of the mode of cooperativity in the rotation relaxations as the tem- perature is raised or lowered across the T_g. At very low temperatures, the isolated structures give non cooperative behavior preventing extrapolation [75]. The difference, $T_c - T_g$, is significant to determine the order in the glassy state. A higher internal stress state is reflected by greater $T_c - T_g$ values. Ibar postulates that the coordinates of the compensation point transcribe the coupling characteristics between different modes of relaxation observed in individual activated processes. Further, Ibar assumed that "entropy increases with increasing disorder", therefore the difference is related to a term Ibar defines as "Degree of Disorder"; See more on this subject in Subsection 6.5. Mano *et al.* [39] interpreted the lack of extrapolation of the lower temperature polarization in infer a β relaxation process. They also argue that the compensation effect is a consequence of the coupling between the different relaxation modes at the glass transition. Sauer *et al.* [76] developed an interpretive scheme (extending Ibar's analysis) to provide a physical relationship between the cooperative and uncooperative motions. When the relaxation motions are localized and uncooperative, the activation energy represents the energy barrier for local motion of an isolated structural unit in the polymer molecule (S and H vary linearly with T). As T approaches T_g from the glassy state, at T near to T_g the motions are more complex, the free volume is not large enough to accommodate all the potential motions at that temperature. The configurational entropy term becomes dominant producing a consequent change in the activation energy. By comparing the activation energies at each depolarization window, the temperature related to the maximum activation energy was designated as T_g by Sauer *et al.* [76].

Critics of the compensation law have attribute the phenomenon to be the result of statistical propagation of error [77] rather than a material property. Tetsseydre and Lacabanne [78] therefore use statistical analysis to determine the validity of T_c. The compensation temperature is related to the measure temperature *via* its harmonic mean as

$$T_{hm} = \langle T_{mi}^{-1} \rangle \tag{24}$$

for 95% confidence in T_c

$$T_c \cong T_c \pm \bar{t}_{N-2,0.975}\sqrt{V(T_c)} \tag{25}$$

$$V = \frac{\sum \left[G_c^*(T_c) - \Delta G_e^*(T_c)\right]^2}{(N-2)\sum(S_i^* - \Delta S^*)^2} \tag{26}$$

where N = number of H, τ_{oi} pairs (number of windows); $\bar{t}$ is the statistical dispersion limit, V is the variance of the estimated T_c, G_e^* is the estimated value of G at T_c. H and S are given by

$$H^* = H_i - kT_{mi} \tag{27}$$

$$S^* = -k\ \ln(\tau_{oi}) + kT_{mi} \tag{28}$$

The claim to that at that point the single relaxation time is fulfilled, is further questioned by Read [79]. He postulates that the linear relationship between the activation enthalpy and activation entropy is a consequence of structural change toward equilibrium with increasing temperature.

Interpretation of global TSD spectra is impeded by the formation of space charge induced relaxations. The space charge peaks are associated with stored charges between crystalline domains in semicrystalline material an due to water or other absorbed impurities in amorphous materials [2]. Determination on whether a relaxation is a space charge effect or a liquid–liquid transition (T_{ll}) are made by annealing the material in the vicinity of the T_{ll} [80]. A decrease in the height of the peaks after extended vacuum drying are other indicators of space charges. The debate over the origins of the multiple peaks occurring in the PLCs is not new. From a big picture standpoint, this debate centers on the existence or non existence of the T_{ll} peak. This must be separated from the PLC materials considered for instance the PET/xPHB copolymers. In this case the assignment of the individual peaks to phases dominated by the non-PLC matrix and the PLC phase are understandable. It is interesting to note than in earlier works on TSD of polystyrene, Lacabanne noted that the occurrence of multiple peaks by internal friction measurements on the torsion braid analyzer coincided with that of the TSD. Lacabanne *et al.* [81] studied the TSD of anionic PS. Through comparison of TSD and torsion braid analysis they concluded the existence of an actual T_{ll} transition.

Differences in experimental technique and data analysis can lead to contradictory results. Thus in the global TSD spectra shown in Figure 3, two transitions for the PET/0.6PHB copolymer are evident. Analysis of the window polarized data for the same copolymer shows only one enthalpy or entropy peak (Figs. 8a, b and c). This dis-

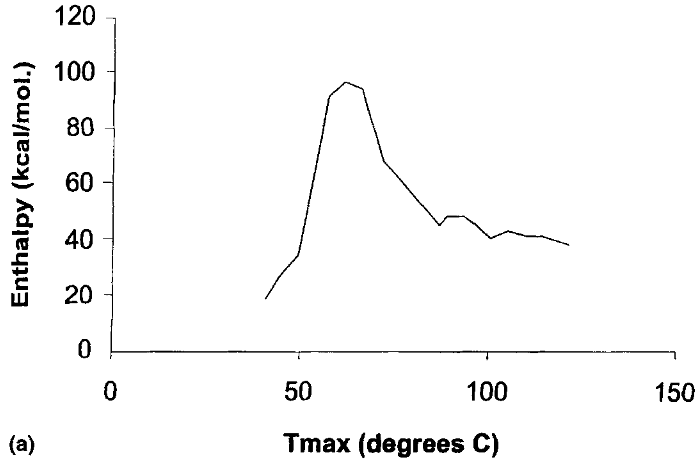

FIGURE 8 Analysis of windows polarization spectra shown in Figure 5. (a) enthalpy–polarization temperature (b) entropy – polarization temperature and (c) enthalpy–entropy relationships.

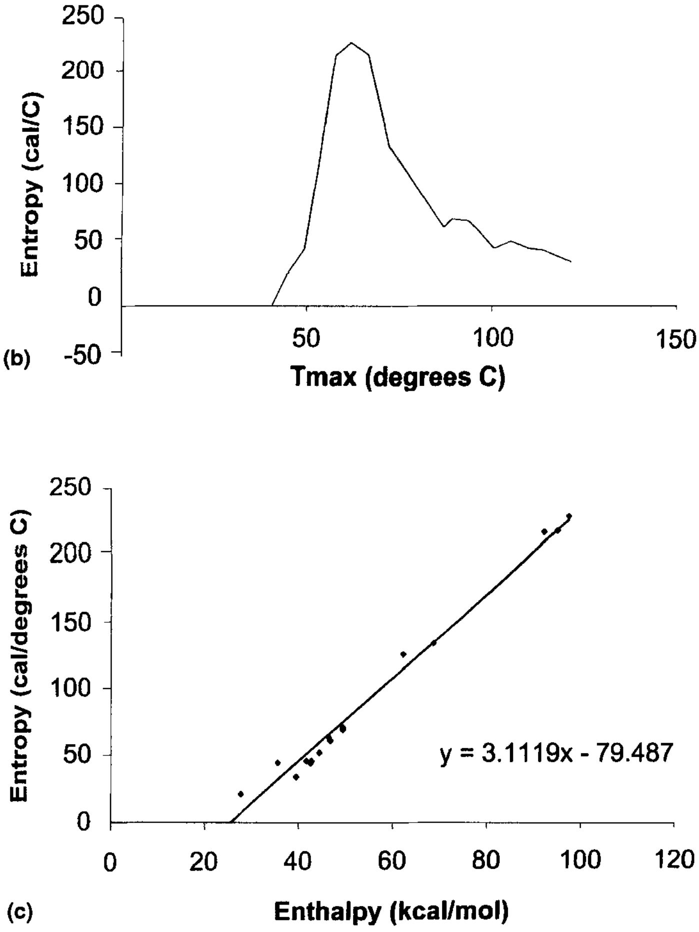

FIGURE 8 (Continued)

crepancy has resulted in assigning the 100°C transition temperature to the space charge effect rather than a polymer transition. One way to distinguish between a space charge transition and a polymer transition is to measure the peak current corresponding to different field strengths. The results are shown in Figure 9a and b. As can be seen the linear dependence in Figure 9b indicates the ohmic and real nature of the transition temperature.

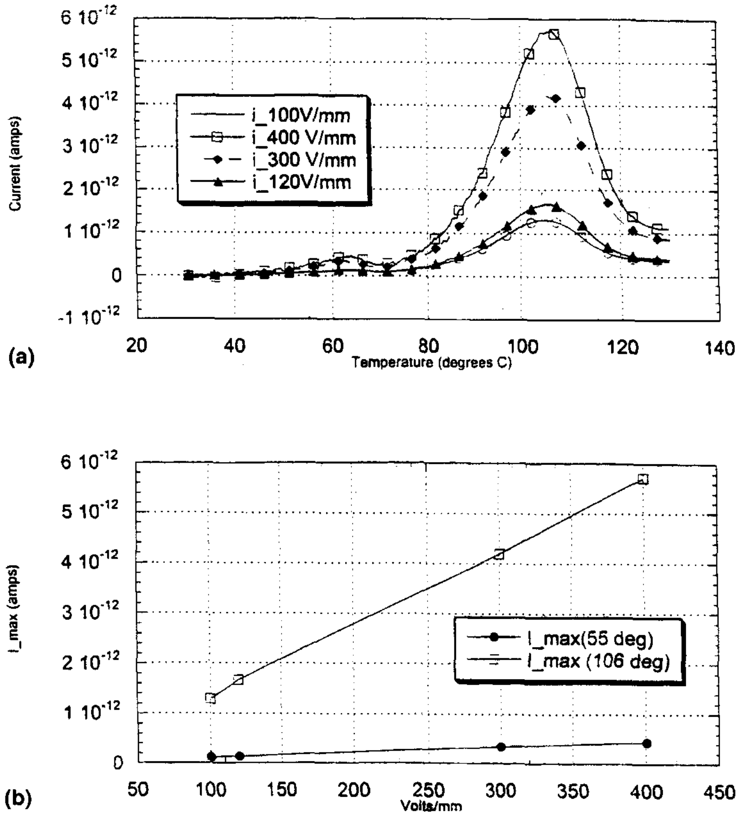

FIGURE 9 (a) Influence of charging field strength on the peak temperatures and currents for the PET/0.6 PHB (b) with the current maxima – temperature relationship showing ohmic behavior.

6. APPLICATIONS OF TSD

6.1. Blends: Relaxations and Phase Diagrams

Plasticization of the peaks is shown by a decreasing peak with increasing plasticizer concentration PVC + NBR blends were studied to determine miscibility. The effect of the dipole–dipole interactions resulted in a decreasing compensation temperature with increasing nitrile content. TSD was useful in determining the level of molecular mixing. The existence of a strict proportionality between $i_{\max}$ and field strength implies uniform dipolar polarization. i_{max} is also linear with butadiene content implying micro-brownian motions of chain segments involving rotation of *cis* and *trans* vinyl butadiene isomers [82]. Application of the compensation law to blends of PVC with chlorinated PE was used to prove incompatibility due to large differences in τ [83].

6.2. Comb Thermotropic PLCs

Simon [24] determined the relaxations of comb PLCs and of blends of a comb PLC with a highly dipolar dye. Since the dielectric behavior of the polymer is determined by the charge distribution and by the statistical thermal motion of the polar groups, the chemical structure strongly affects the strength of the relaxation. Thus polymers having polar groups on their main chain or in side groups have high dielectric permittivity [84]. He [24] utilized the technique to interpret the persistent orientational ordering of the polymer at $T > T_g$. Following his work, a few other investigators have also examined side chain LCs with TSD [85-88].

Mano *et al.* [89] studied thermotropic liquid crystalline polymers having side-chain mesogenic groups of acrylate, methacrylate and siloxane backbones. In previous dielectric studies two relaxations in these systems had been determined using calorimetry. The low frequency relaxation had a narrow peak similar to relaxations involving rotations about the short molecular axis in low molecular mass liquid crystals.

This feature is not endemic to all side chain PLCs as Mano *et al.* [90] and Kohler [91] found. For a sPLC they found that the i_{max} increased with increasing field strength (E_p) for low field strengths but for higher values of field strength, i_{max} decreased with increasing E_p. This behavior was ascribed to the detrapping of ionic impurities and/or homocharges at higher voltages, with the consequence that the motion of charges through the sample would make dipolar orientation a function of the field due to motion of space charges.

The greater sensitivity of the TSD over DSC is evidenced by Mano *et al.*, work on poly *n*-hexyl isocyanate sPLCs [89, 90]. Contrary to the single relaxation depicted by DSC, the TSD spectra detected three regions where the peaks scaled linearly with field strength. It was therefore possible to separate relaxations of the main chains from the mesogenic side groups. In their studies of a sPLC having published T_g

of −7°C and a smectic *C*-isotropic transition ($T_{s\text{-iso}}$) at 77°C, they found additional peaks at 8 and 31°C. Plots of $i_{\max}$ *v/s* E_p were straight lines for all three transitions indicating the dipolar nature of the corresponding relaxation processes. Since relaxations due to space charge motions are weakly dependent on E_p and susceptible to electret formation, intensity of peaks is sensitive to the presence of strong dipoles of the cyano group and related to the motions of the mesogenic group around the main chain or higher mobility of the side chain and molecular volume.

TSD has also been successful in showing the anisotropic nature of dipoles in sPLCs [88]. The multiple peaks evident in side chain PLCs have been ascribed to the motions involving the longitudinal and transverse dipole moments of the mesogenic side group. In experiments with side chain PLCs, the sensitivity of TSD over DSC was again apparent, with more transitions between T_g and $T_{s\text{-iso}}$ detected. All peaks scaled linearly with field strength, indicating dipole relaxations rather than space charge induced peaks.

The height of the TSD spectra is proportionate to the mobility of the relaxation strength. As Ronach and Testard [92] explain, low temperature relaxations arise from low-amplitude motions which occur around the available free volume cause the relaxations to be characterized by low intensity discharges, by small activation enthalpies and by negligible activation entropies. The breadth is related to the spacer length especially for the side chain PLCs arises from the increased number of possible conformations due to increased methylene groups and leads to reorientation of the side chain group. The breadth of the relaxation for smaller spacers ($n = 3, 4$) is smaller than for $n = 10$.

6.3. Thermotropic Longitudinal PLCs

In one of the early investigations of TSD, Brostow *et al.* [25] found that for a PET/0.6 PHB, two peaks were found: one at 65°C and the other at 101°C, referred to as α and α' peaks respectively. Their results were supported by dielectric studies done on the same systems by Gedde *et al.* [93]. Since the α relaxation of PET is $\cong$69°C, the α transition was interpreted to be related to the PET phase. The α' peak was interpreted to be related to the onset of crystallization of PET which takes place at 100°C. Keeping the field strength constant, it was found that changing T_p from 50 to 140°C resulted in a proportionate increase of the α peak till $T_p = 90°C$; the height of the α' peak remained unchanged. Thus implying a dielectric relaxation maximum at 90°C. Keeping the $T_p = 90°C$, the effect of the field strength was studied. It was found that the effect of increasing E_p had the same effect as changing T_p with one exception, the α peak was present for all E_p's. Polarizing at $T_p < T_g$; resulted in moving the α transition to 80°C. As the value of T_p was taken to temperatures greater than α', the α transition peak was ameliorated due to an increase in cold crystallization at higher temperatures. Sauer conducted tests on a variety of PLC systems and established the effects of matrix morphology in relationship to PLC architecture [30].

Shinn *et al.*, determined the block structure for copolymers made for polyethylene terephthalate-*p*-acetoxybenzoic acid made from low and high molecular weight PET using TSD. Traditional block copolymerization equations were related to the TSD spectra through the use of Eqs. (7) and (8). The equations were weighted based on mole percent of feed material. It was found that block copolymers formed from lower molecular weight PET had greater blockiness in comparison to copolymer containing the higher molecular weight PET.

In using TSD for main chain polymer liquid crystals, the different states of order require cautious use of the compensation plots. Collins and Long [19] studied films of the commercial Vectra (Hoechst Celanese) material. He found a large degree of cooperativity above the T_g (when defined as the temperature related to the peak in enthalpy-T_p plot).

6.4. Annealing and Physical Aging Effects

The use of the TSD technique in aging studies has been described by Struik [94, 95]. Brostow *et al.* [25] investigated the effect of the sequence in TSC experimentation. By keeping $T_p = 90°C$ (previously determined to be the temperature at which the maximum current was produced for the relaxation). As the time at the polarization temperature was increased (in the absence of the polarizing field), i_{max} decreased.

Crine applied his compensation law formulation to the problem of dielectric aging of polyethylene. He found that the free energy of PE thermally aged above its melting point varied linearly with antioxidant contents. Physical aging of PMMA was interpreted using a series of annealing experiments where $T_{\text{anneal}} \ll T_g$; and $T_p = T_{\text{anneal}}$ for varying times. Depolarization currents were measured in both the T_g and the β regions. It was found that as annealing time increase the $i_{\max}$ decreased for both the relaxations.

6.5. Electro, Optical and Ferroelectric Applications

Given that ferroelectrics have switchable polarization at the Curie temperature, the TSD technique is showing great promise as ferroelectric polymers develop [96]. Extensive use of TSD in ferroelectric materials has been conducted [97, 98]. A correlation between Curie temperatures and compensation temperatures lent credence to the concept of using compensation law with TSD data. TSD has shown complementary information to impedance spectroscopy for sodium silicate glass [99]. Dye doping of poly (vinyl butyrate) has been analyzed by TSD. Low dye concentrations resulted in lower $T_{\max}$, higher $i_{\max}$ and higher activation energies, due to formation of charge transfer complexes [100]. Annealing effects on the pyroelectric coefficient were determined using TSD by Teyssèdre *et al.* [101].

The relaxation behavior of polymers has become even more pertinent in the case of optical device technologies [102]. Doping PMMA with aniline derivatives causes relaxation behavior analogous to plasticization: decreased transition temperatures with increasing doping level. With increasing doping level, more dopants disorient in a manner controlled by doping level. Separation based on whether the interaction is of a "dipole–dipole" nature is made based on its energy value (0.2 eV).

A combination of photocurrent and TSC [103] was used on epoxy films to elucidate the mechanical stress effects. Under mechanical stress, the photocurrent for a positive bias on the illuminated electrode was larger than under negative bias. TSD behavior in the absence of luminescence also showed similar trends.

6.6. Orientation Effects

Combination of DSC and TSD has been effectively used by Bernes *et al.* [104] to study the orientation effects in a PET homopolymer. It was possible to isolate the cause of the exotherm observed in the unoriented PET in the constant heating cycle as being related to the amorphous phase with delocalized cooperative movements. Upon uniaxial orientation the amorphous phase becomes more ordered. Lindner [105] postulated that these "ordered" amorphous quantities had short range nematic order. Biaxial orientation transforms these "ordered" amorphous regions into crystalline domains. These conclusions could be based on the DSC experiments alone. However comparing TSDs of the PET having $T_p = T_g$, the sub T_g relaxation at 60°C could then be traced as originating solely from the amorphous region. This orientation effect on the relaxation can also be attributed to a minimization of defects. In condensed systems the overall response of the material to the application of an external field is also determined by the local inhomogenities in the structure. Lacabanne *et al.* [106] report the effects of molecular orientation on PET amorphous and biaxially oriented film and found no change in T_c. However the width of the distribution in amorphous PET is greater than the width in biaxially oriented PET. For PEEK, Mourgues-Martin *et. al.* [107] report that the crystallinity changes did not affect the $T_c - T_g$ as would be expected from Ibars "Degree of Disorder" approach. However as the crystallinity increased, the relaxation distribution function decreased. For polycarbonate changes between a quenched and annealed sample, Bernes *et al.* [108] found that two relaxation modes develop upon annealing. The variance in the distribution function and the formation of two relaxation modes upon annealing has been attributed to the "constrained amorphous phase" [109] and the "rigid amorphous phase" [110]. The effect of biaxially oriented film is most strongly evidenced through differences in the TSPC and TSDC for the film [111], due to the absence of the preliminary heating stage.

Acknowledgements

The author acknowledges with appreciation TherMold Partners, Inc., Stamford CT for providing equipment and technical support. Comments and suggestions of Bryan Bilyeu, University of North Texas and a referee are also sincerely appreciated.

References

[1] Carr, S. H. (1982). In: *Electrical Properties of Polymers*, Edited by Seanor, D. A., Chapter 5, Academic Press, New York.

[2] van Turnhout, J. (1975). *Thermally Stimulated Discharge of Polymer Electrets*, Elsevier, Amsterdam.

[3] Eguchi, M. (1925). *Phil. Mag.*, **49**, 178.

[4] Eguchi, M. (1922). *Japan J. Phys.*, **1**, 10.

[5] Frei, H. and Groetzinger, G. (1936). *Physics*, **Z37**, 720.

[6] Vaderschueren, J. and Gasiot, J. (1979). In: *Thermally Stimulated Relaxation in Solids*, Edited by Bräunlich, P., Chapter 4, Springer-Verlag, Berlin-Heidelberg-New York.

[7] Gross, B. (1949). *J. Chem. Phys.*, **17**, 866.

[8] Wikstroem, S. (1953). *Ericsson Tech.*, **9**, 225.

[9] Gubkin, A. N. and Matsonashvili, B. N. (1962). *Fiz. Tverd. Tela*, **4**, 1196.

[10] Murphy, P. V. (1963). *J. Phys. Chem. Sol.*, **24**, 329.

[11] Bucci, C. and Fieschi, R. (1964). *Phys. Rev. Lett.*, **12**, 16.

[12] van Turnhout, J. (1980). In: *Electret*, Edited by Sessler, G., Chapter 3, Springer, Berlin.

[13] Bernes, A., Boyer, R. F., Chatain, D., Lacabanne, C. and Ibar, J. P. (1987) In: *Order in the Amorphous State of Polymers*, Edited by Keitnath, S. E., p. 305, Plenum, New York.

[14] Gourari, A., Bendaoud, M., Lacabanne, C. and Boyer, R. F. (1985). *J. Polymer Sci. Phys.*, **23**, 889.

[15] Vanderschueren, J., Linkens, A., Haas, B. and Dellicour, E. (1978). *J. Macromol. Sci. Phys.*, **B15**, 449.

[16] Frank, B., Prünbing, P. and Pissis, P. (1996). *J. Polymer Sci. Phys.*, **34**, 1853.

[17] Boye, J., Demont, P. and Lacabanne, C. (1994). *J. Polymer Sci. Phys.*, **32**, 1359.

[18] Lavergne, C., Dutresne, A., Chatain, D. and Lacabanne, C. (1993). *J. Therm. Anal.*, **40**, 705.

[19] Su, W. F. A., Carr, S. H. and Brittain, J. O. (1980). *J. Appl. Polymer Sci.*, **25**, 1355.

[20] Müller, P. (1974). *Phys. Status Solidi*, **A23**, 165.

[21] Vandershueren, J., Niezette, J., Yianakopolos, G. and Thielen, A. (1991). *Thermochim. Acta*, **192**, 287.

[22] Lacabanne, C. (1974). *Ph.D. Thesis*, University of Toulouse, France.

[23] Chatain, D. (1974). *Ph.D. Thesis*, University of Toulouse, France.

[24] Simon, G. (1989). *Polymer*, **30**, 2227.

[25] Brostow, W., Kaushik, B. K., Mall, S. B. and Talwar, I. M. (1992). *Polymer*, **33**, 4687.

[26] Brostow, W., Callahan, R., D'Souza, N. A. and Galop, M. (1997). *Proceedings of the Annual Technical Conference Society of Plastics Engineers*, **54**, 1881.

[27] Chen, D. and Zachman, H. G. (1991). *Polymer*, **32**, 1612.

[28] Cao, M. Y., Varma-Nair, M. and Wunderlich, B. (1990). In: *Polymers for Advanced Technologies*, **1**, 151.

[29] Sauer, B. B., Dipaolo, N. V., Avakian, P., Kampert, W. G. and Starkweather, H. W. Jr. (1993). *J. Polymer Sci. Phys.*, **31**, 1851.

[30] Sauer, B. B., Beckerbauer, R. and Wang, L. (1993). *J. Polymer Sci. Phys.*, **31**, 1861.

[31] Brostow, W. and Samatowicz, D. (1993). *Polymer Eng. & Sci.*, **33**, 581.

[32] Brostow, W., Hess, H. and López, B. (1994). *Macromolecules*, **27**, 2262.

[33] Damman, S. B., Mercx, F. P. M. and Lemstra, P. J. (1993). *Polymer*, **34**, 2726.

[34] Damman, S. B. and Buijs, J. A. H. M. (1994). *Polymer*, **35**, 2359.

[35] Matthiesen, A., McIntyre, F. and Ibar, J. P. (1991). *Food Technology*, July, p. 106.

[36] Dias, A. B., Correia, N. T., Moura Ramos, J. J. and Fernandes, A. C. (1994). *Polymer Int.*, **33**, 293.

[37] Dias, A. B., Moura Ramos, J. J. and Williams, G. (1994). *Polymer*, **35**, 1253.

[38] Bucci, C., Fieschi, R. and Guidi, G. (1966). *Phys. Rev. B*, **148**, 816.
[39] Moura Ramos, J. J., Mano, J. F. and Nestor, G. (1996). *J. Polymer Sci. Phys.*, **34**, 2067.
[40] Ibar, J. P., Denning, P., Thomas, T., Bernes, A., De Goys, C., Saffell, J. R., Jones, P. and Lacabanne, C. (1990). In: *Polymer Characterization: Physical Property, Spectroscopic and Chromatographic Methods*, Edited by Provder, T. and Craver, C. D., Chapter 10, American Chemical Society.
[41] Ibar, J. P. (1991). *Polymer Eng.* and *Sci.*, **31**, 1467.
[42] Ibar, J. P. (1991). *Thermochim. Acta*, **192**, 91.
[43] Ibar, J. P. (1991). *Thermochim. Acta*, **192**, 265.
[44] Ibar, J. P. (1991). *Thermochim. Acta*, **192**, 297.
[45] Jonscher, A. K. (1977). In: *Thermally Stimulated Processes in Solids: New Prospects*, Edited by Fillard, J. P. and van Turnhout, J., p. 53, Elsevier, Amsterdam, Oxford, New York.
[46] Pfister, G. and Abkowitz, A. (1974). *J. Appl. Phys.*, **45**, 1001.
[47] McKeever, S. W. S. and Hughes, D. M. (1975). *J. Phys. D*, **8**, 1520.
[48] Moran, P. R. and Fields, D. E. (1974). *J. Appl. Phys.*, **45**, 3266.
[49] Manifacier, J. C., Gasiot, J., Parot, P. and Fillard, J. P. (1978). *J. Phys.*, **C11**, 1011.
[50] Vanderschurern, J., Linkens, A., Gasiiot, J., Fillard, P. and Parot, P. (1980). *J. Appl. Phys.*, **52**, 4967.
[51] Mizutani, T., Suzoki, Y. and Ieda, M. (1977). *J. Appl. Phys.*, **8**, 8.
[52] Barandiarán, J., Del Val, J. J., Lacabanne, C., Chatain, D., Millán, J. and Martínez, G. (1983). *J. Macromol. Sci. Phys.*, **B22**, 645.
[53] del Val, J. J., Alegría, A., Colmenero, J. and Lacabanne, C. (1986). *J. Appl. Phys.*, **59**, 3829.
[54] del Val, J. J., Alegría, A., Colmenero, J. and Barandiarán, J. M. (1986). *Polymer*, **27**, 1771.
[55] Monpagens, J. C., Chatain, D. and Lacabanne, C. (1977). *Electrostatics*, **3**, 87.
[56] Lacabanne, C., Chatain, D. and Monpagens, J. C. (1977). *J. Macromol. Sci. Phys.*, **B13**, 537.
[57] Colmenero, J., Alegria, Alberdi, J. M., del Val, J. J. and Ucar, G. (1987). *Phys. Rev.*, **B35**, 3995.
[58] del Val, J. J., Alegría, A., Colmenero, J. and Barandiarán, J. M. (1986). *Polymer*, **27**, 1771.
[59] Lacabanne, C., Chatain, D., Mopagens, J. C., Hiltner, A. and Baer, E. (1978). *Solid State Communications*, **27**, 1055.
[60] Lawson, A. W. (1957). *J. Chem. Phys. Solids*, **3**, 250.
[61] Lawson, A. W. (1960). *J. Chem. Phys.*, **32**, 131.
[62] Keyes, R. W. (1958). *J. Chem. Phys.*, **29**, 467.
[63] Eby, R. K. (1962). *J. Chem. Phys.*, **37**, 2785.
[64] Hoffman, J. D., Williams, G. and Passaglia, E. (1966). *J. Polymer Sci. C*, **14**, 173.
[65] Crine, J. P. (1984). *J. Macromol. Sci. Phys.*, **B23**, 201.
[66] Crine, J. P. (1989). *J. Appl. Phys.*, **66**, 1308.
[67] Glasstone, S., Laidler, K. J. and Eyring, H. (1941). *The Theory of Rate Processes*, McGraw Hill, New York.
[68] Warfield, R. W. (1974). *Makromol. Chem.*, **175**, 3285.
[69] Sharma, B. K. (1979). *Acoustica*, **43**, 225.
[70] Sharma, B. K. (1981). *Acoustica*, **48**, 118.
[71] Sharma, B. K. (1982). *J. Phys.*, **D15**, 1273.
[72] Moura Ramos, J. J., Mano, J. F. and Sauer, B. B. (1997). *Polymer*, **38**, 1081.
[73] Zielinski, M., Swiderski, T. and Kryszewski, M. (1978). *Polymer*, **19**, 883.
[74] Cost, J. R. (1983). *J. Appl. Phys.*, **54**, 2137; Aldana, M., Laredo, E., Bello A. and Suarez, N. (1994). *J. Polymer Sci. Phys.*, **32**, 2197.
[75] Collins, G. and Long, B. (1994). *J. Appl. Polymer Sci.*, **53**, 587.
[76] Sauer, B. and Avakian, P. (1992). *Polymer*, **33**, 5128.

[77] Krug, R. R., Hunter, W. G. and Grieger, R. A. (1976). *J. Phys. Chem.*, **80**, 2341.
[78] Tessèdre, G. and Lacabanne, C. (1995). *J. Phys. D*, **28**, 1478.
[79] Read, B. E. (1989). *Polymer*, **30**, 1439.
[80] Boyer, R. F. (1980). *Macromol. Sci. Phys.*, **B18**, 461.
[81] Lacabanne, C., Goyard, P. and Boyer, R. F. (1990). *J. Polymer Sci. Phys.*, **18**, 277.
[82] Vandershueren, J., Ladang, M. and Heuschen, J. M. (1980). *Macromolecules*, **13**, 973.
[83] del Val, J. J., Colmenero, J. and Lacabanne, C. (1988). *Solid State Communications*, **69**, 707.
[84] Hedvig, P. (1977). *Dielectric Spectroscopy of Polymers*, John Wiley and Sons, New York.
[85] Faubertt, F., Gilli, J. M., Sixou, P., Dandurand, J. and Lacabanne, C. (1990). *Mol. Cryst. Liq. Cryst.*, **178**, 133.
[86] Mano, J. F., Moura Ramos, J. J. and Williams, G. (1994). *Polymer*, **35**, 5170.
[87] Mano, J. F., Correia, N. T., Ramos, J. J. and Fernandes, A. C. (1995). *J. Polymer Sci. Phys.*, **33**, 269.
[88] Mano, J. F., Correia, N. T., Ramos, J. J. and Coates, D. (1995). *Macromol. Chem. Phys.*, **196**, 2289.
[89] Mano, J. F., Correia, N. T. and Ramos, J. J. M. (1994). *Polymer*, **35**, 3561.
[90] Mano, J. F., Moura Ramos, J. J., Fernandes, A. and Williams, G. (1994). *Polymer*, **35**, 5170.
[91] Köhler, W., Robello, D. R., Dao, P. T., Willand, C. S. and Williams, D. (1990). *J. Chem. Phys.*, **93**, 9157.
[92] Ronarch, D. and Testard, O. (1982). *J. Phys. Sci. Instru.*, **15**, 636.
[93] Gedde, U. W., Buerger, D. and Boyd, R. H. (1987). *Macromolecules*, **20**, 988.
[94] Struik, L. C. E. (1978). *Physical Aging in Amorphous Polymers and Other Materials*, Elsevier, Amsterdam.
[95] Struik, L. C. E. (1986). In: *Failure of Plastics*, Edited by Brostow, W. and Corneliussen, R., Chapter 11, Hanser. Munich.
[96] Nalwa, H. S. (1995). *Ferroelectric Polymers: Chemistry, Physics and Applications*, Marcel Dekker, Inc., New York, Basel, Hong Kong.
[97] El Hout, J., Chatain, D., Lacabanne, C., Montaner, A. and Galtier, M. (1989). *Makromol. Chem. Symp.*, **24**, 129.
[98] Teyssedre, G., Bernes, A. and Lacabanne, C. (1995). *J. Polymer Sci. Phys.*, **33**, 879.
[99] Giuntini, J. G., Vanderschueren, J., Zanchetta, J. V. and Henn, F. (1994). *Phys. Rev.*, **B50**, 12, 489.
[100] Chand, S. and Kumar, N. (1995). *J. Mat. Sci. Lett.*, **14**, 142.
[101] Teyssèdre, G., Bernes, A. and Lacabanne, C. (1993). *J. Thermal Anal.*, **40**, 711.
[102] Zheng, G., Xu, Y., Wang, W., Feng, Z., Wang, X. and Wen, J. (1994). *Polymer Int.*, **35**, 273.
[103] Kawamoto, A., Suzuoki, Y., Ikejiri, T., Mizutani, T. and Ieda, M. (1988). *IEEE Trans. Elec. Insulation*, **23**, 201.
[104] Bernes, A., Chatain, D. and Lacabanne, C. (1992). *Thermochim. Acta*, **204**, 69.
[105] Lindner, W. L. (1973). *Polymer*, **14**, 9.
[106] Lacabanne, C., Lamure, A., Teyssedre, G., Bernes, A. and Mourgues, M. (1994). *J. Non-Cryst. Solids*, **172**, 884.
[107] Mourgues-Martin, M., Bernes, A. and Lacabanne, C. (1993). *J. Thermal Anal.*, **40**, 697.
[108] Bernes, A., Martinez, J. J., Chatain, D. and Lacabanne, C. (1991). *J. Thermal Anal.*, **37**, 1795.
[109] Boyer, R. F. (1977). In: *Encylopoedia of Polymer Science and Technology II*, p. 745.
[110] Cheng, S. Z. T., Pan, R. and Wunderlich, B. (1988). *Makromol. Chem.*, **189**, 244.
[111] Thielen, A., Cerfontaine, J., Nietzette, J., Feyder, G. and Vandershueren, J. (1994). *J. Appl. Phys.*, **76**, 4696.